Formation and Characterization of Organic Monolayers on Semiconductor Surfaces

Robert J. Hamers

Department of Chemistry, University of Wisconsin at Madison, Madison, Wisconsin 53706; email: rjhamers@wisc.edu

Annu. Rev. Anal. Chem. 2008. 1:707–36

First published online as a Review in Advance on March 21, 2008

The *Annual Review of Analytical Chemistry* is online at anchem.annualreviews.org

This article's doi:
10.1146/annurev.anchem.1.031207.112916

1936-1327/08/0719-0707$20.00

Key Words

silicon, biosensors, interfaces, microelectronics, infrared spectroscopy, scanning tunneling microscopy (STM)

Abstract

Organic-semiconductor interfaces are playing increasingly important roles in fields ranging from electronics to nanotechnology to biosensing. The continuing decrease in microelectronic device feature sizes is raising an especially great interest in understanding how to integrate molecular systems with conventional, inorganic microelectronic materials, particularly silicon. The explosion of interest in the biological sciences has provided further impetus for learning how to integrate biological molecules and systems with microelectronics to form true bioelectronic systems. Organic monolayers present an excellent opportunity for surmounting many of the practical barriers that have hindered the full integration of microelectronics technology with organic and biological systems. Of all the semiconductor materials, silicon and diamond stand out as unique. This review focuses upon the preparation and characterization of organic and biomolecular layers on semiconductor surfaces, with special emphasis on monolayers formed on silicon and diamond.

1. INTRODUCTION

Organic-semiconductor interfaces are playing increasingly important roles in fields ranging from electronics to nanotechnology to biosensing (1–5). The continuing decrease in microelectronic device feature sizes is raising especially great interest in understanding how to integrate molecular systems with conventional, inorganic microelectronic materials, particularly silicon. The explosion of interest in the biological sciences has provided further impetus for learning how to integrate biological molecules and systems with microelectronics to form true bioelectronic systems. Yet, practical barriers to such an integration remain due to the inherent instability of silicon and most other semiconductors in aqueous environments.

Organic monolayers present an excellent opportunity for surmounting many of the practical barriers that have hindered the full integration of microelectronics technology with organic and biological systems. Monolayers comprised simply of alkyl chains can act as nearly impervious barriers to aqueous media due to their hydrophobic nature. Thin monolayers can act either as electrically resistive layers or as conductive layers, depending on the nature of the bonding within the layers.

Of all the semiconductor materials, silicon and diamond stand out as unique; monolayers on these materials are consequently the most widely studied and therefore constitute the primary emphasis of this review. Silicon is of paramount importance because it is the foundation of the microelectronics field and is likely to remain so for the foreseeable future. Diamond is an especially appealing material because in addition to being the hardest substance known, it is also remarkably stable in harsh chemical and electrochemical environments; this makes it a nearly ideal material for applications involving exposure to wet environments, especially those involving biological biomolecules. Here, I present a selective review of the formation and characterization of organic monolayers, with an emphasis on monolayers formed on silicon and diamond.

2. FORMATION OF ORGANIC MONOLAYERS ON SEMICONDUCTOR SURFACES

The formation of well-defined organic layers on silicon and other semiconductors typically follows one of two routes. Modification by adsorption in vacuum most commonly begins with "clean" surfaces that are often prepared by annealing under ultrahigh vacuum conditions. The formation of a free surface leaves the surface atoms with low coordination numbers and typically leads to unsaturated "dangling bonds" at the interface. The semiconductor surfaces undergo atomic rearrangements (also called reconstructions) to reduce the number of exposed dangling bonds, but in most cases the resulting surfaces remain highly reactive. Grafting of molecular layers under ambient conditions typically involves first passivating the surfaces via either wet-chemical or plasma methods, which produces surfaces in which the unsaturated dangling bonds are terminated with hydrogen, chlorine, or another substituent that reduces the reactivity to facilitate handling in ambient conditions. This process must then be followed by reaction with the organic molecule of interest.

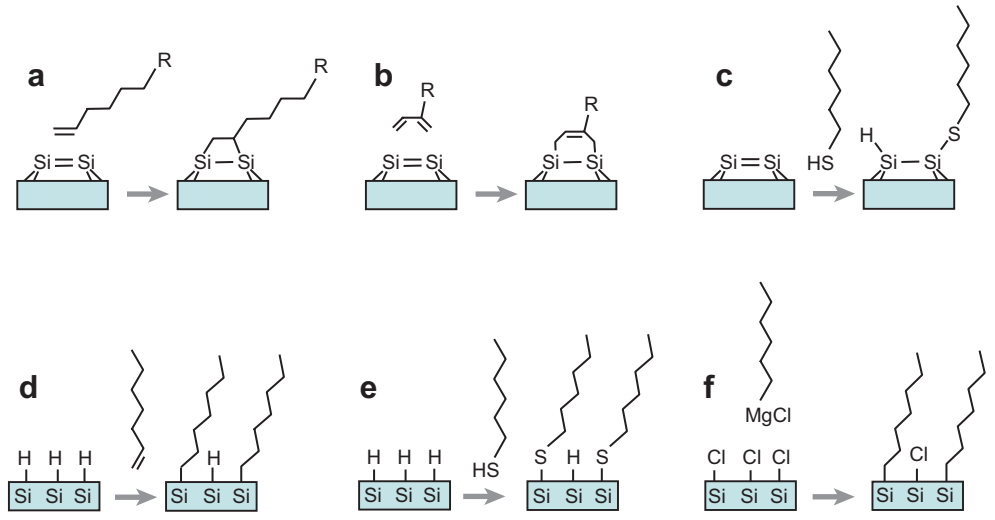

Figure 1

Commonly used methods for forming organic monolayers on semiconductor surfaces. Panels *a–c* depict methods used in ultrahigh vacuum studies, where the starting surfaces are clean. Panels *d–f* depict methods used in ambient conditions on hydrogen-passivated or halogen-passivated surfaces.

Figure 1 presents some of the most commonly used methods for forming organic monolayers. **Figure 1*a–c*** depicts methods used in ultrahigh vacuum studies, where the starting surfaces are clean. The precise arrangements of atoms depend on the semiconductor and the specific crystal face; those shown in **Figure 1*a–c*** are appropriate for the (001) surfaces of silicon, diamond, and germanium, which share a common bonding motif. **Figure 1*d–f*** depicts methods used in ambient conditions on hydrogen-passivated or halogen-passivated surfaces; most of these studies have been performed using silicon, although recent studies have extended these methods to diamond and other semiconductors.

2.1. Formation of Semiconductor-Organic Monolayers in Vacuo

In ultrahigh vacuum, the most widely studied surface has been the (001) crystal face of silicon, as it represents the starting point for virtually all silicon-based microelectronic devices. The (001) surfaces of silicon, germanium, and the diamond allotrope of carbon all undergo surface reconstructions in which adjacent atoms move toward one another, forming dimers (6–8). Because the bulk-truncated surfaces have two broken bonds per atom, the formation of the dimers is, to a first approximation, a rehybridization of these two dangling bonds to allow formation of a Si=Si, C=C, or Ge=Ge double bond at the surface. Although this description is vastly oversimplified, it highlights the fact that there are important conceptual connections between these surfaces and the more common C=C, Si=Si, and Ge=Ge bonds of organic and organometallic compounds (9, 10). Of particular interest has been the

desire to use bond-forming reactions, such as the well-known cycloaddition reactions of organic chemistry, in order to facilitate a wider array of surface modifications (11–39).

The reaction between organic alkenes and the (001) face of silicon, germanium, and diamond appears similar to a [2+2] cycloaddition reaction, in which two electrons from the C=C π bonds of the reactant molecules and two electrons from the π bond of the surface dimers link together in a pericyclic manner, thereby linking each molecule to the surface with two bonds and forming a four-member ring at the interface (**Figure 1*a***) (15). A second type of reaction, technically equivalent to a [4+2] Diels-Alder reaction, can also take place if there are conjugated double bonds present in the reactant molecule. For example, four electrons of the molecule and two electrons of the substrate interact to form a six-member ring at the interface (shown in **Figure 1*b***) (21–24, 30, 40).

The [2+2], [4+2], and other cycloaddition reactions represent important pathways for organic monolayer formation on silicon and other semiconductors. An important practical feature of this approach is the fact that these are pure addition reactions, so there is no cleavage of C–H or other bonds nor any byproducts other than the simple coupling. This feature makes these reactions ideally suited to formation of well-defined monolayers at room temperature and below. Because the (001) surfaces of Si, Ge, and C (diamond) consist of dimers, the formation of two covalent bonds between each molecule and the underlying surface also implies that when the molecules are linked to the surface, the orientation of the underlying dimers is translated into the orientation of the upper molecular layer. By choosing small cyclic molecules that are highly symmetric and relatively rigid, it is possible to fabricate molecular layers that are essentially epitaxial with the underlying silicon substrate (19, 41).

One interesting aspect of these cycloaddition reactions has been gaining an understanding of the reaction mechanisms, as well as identifying to what extent the well-known Woodward-Hoffman symmetry rules can apply at a surface (42). For typical alkenes, the reaction between two alkenes is forbidden in the highest-symmetry geometry, in which one molecular approaches another from the top. However, the C=C, Si=Si, and Ge=Ge dimers that form on silicon are distorted away from planar configurations. These distorted configurations lead to increased radical character and also facilitate low-symmetry reaction pathways that are not subject to Woodward-Hoffman symmetry rules (14, 21, 30). The [2+2] reactions of simple alkenes with Si=Si and Ge=Ge dimers occur with a reaction probability close to unity (15, 18–20, 39, 43). The reactions on diamond are less favorable, requiring significantly greater exposure (17). Nevertheless, reactions do occur on all three surfaces.

Another class of reaction, the reaction of a 1,3-diene with these surfaces, has also been investigated. This reaction is formally equivalent to a concerted [4+2] (Diels-Alder) reaction. Although normal alkenes react easily with 1,3-dienes but not with other simple alkenes (due to the aforementioned symmetry constraints), it was originally expected that the Si, Ge, and diamond surfaces would exhibit a similar preference (23, 40). Because the surface distortions render the [2+2] reaction (involving a single C=C bond reacting with the surface) unexpectedly facile, in practice the reaction of 1,3-dienes with these surfaces leads to multiple products that include both [2+2]

reaction products (i.e., reaction via a single C=C bonds) and reaction via the [4+2] route (21, 30, 44). Consequently, it is now recognized that the formation of well-organized monolayers is generally more successful when using simple alkenes, except perhaps in the case of diamond (25, 45, 46, 99). Whereas most studies have focused on linking simple hydrocarbons to the surface, the ideas above have been extended to include other types of unsaturated bonds, including carbonyl groups (47).

The formation of molecular layers incorporating conjugated π–electron structures has also been of great interest, in part because electron transfer through π-conjugated systems is expected to be more facile than through saturated organic systems (3). Benzene itself bonds to the surface via a number of different configurations (48–51). Simple substitution to form toluene and/or xylenes leads to further disruption of the structure (11). However, if there is a secondary reactive group present, in most cases the organic monolayers use these groups to bond to the surface, leaving the aromatic character intact. The most notable example is styrene, which reacts almost completely via the C=C group external to the aromatic ring, leaving the π conjugation within the ring intact. Other variants, such as phenyl isothiocyanate (12) and benzonitrile (52–54) also preferentially link through the external substituent.

On the basis of these studies, a number of generalizations can be made. The first is that the reactivity of clean silicon and germanium surfaces in vacuum is sufficiently high that almost any molecule within a reactive group, including simple C=C bonds, will react with the surfaces. Thus, the key question in forming well-defined monolayers becomes one of controlling the overall selectivity of reaction. Because they have only one reactive group, simple alkenes provide the best-defined layers. Dienes and other molecules bearing more than one unsaturated group generally leave poorly defined layers, due to the competition between [4+2] and [2+2] reactions. However, molecular-bearing aromatic groups have a much higher propensity to adopt a well-defined structure that preserves the aromaticity.

A second class of reactions in vacuo involves simple functional groups, such as the thio, amino, and hydroxy groups, which have labile hydrogen atoms that can be easily removed, allowing the S, N, or O atom to link to the semiconductor. Following extensive studies on self-assembled monolayers on metals, many experiments have focused on thiol groups interacting with silicon (55) and other semiconductors such as GaN (56), InP (57, 58), and GaAs (59–62). In each case, bonding to the surface necessitates cleavage of an S–H, N–H, or O–H bond, with the hydrogen remaining bound to the surface. This approach can also be used to link aromatic systems to semiconductor surfaces using reactants such as benzenethiol (55), phenol (63), and aniline (64, 65).

Although most investigations of monolayer formation in vacuo started with highly reactive clean surfaces, a number of studies have investigated reactions with hydrogen-terminated surfaces, in which the undercoordinated surface bonds are bonded to H atoms. These H-passivated surfaces are much less reactive than the clean surfaces; consequently, most molecules will react selectively where the H-passivation has been eliminated. Local desorption of hydrogen can be achieved by low-energy electrons, such as those emitted from the tip of a scanning tunneling microscope. The initiation of a single reaction leads to a propagation of the reaction: As the reaction proceeds via

a radical intermediate in which a molecular radical state is able to abstract an H atom from the adjacent dimer, its reactivity toward subsequent molecules is thereby greatly enhanced. This suggests the possibility of making a variety of extended molecular structures (66).

Studies of monolayer formation on Si(111)-(7 × 7) have also been conducted. On Si(111), the large amount of charge transfer that occurs between different atoms within the unit cells allows reactions to proceed via a diradical pathway (67).

2.2. Formation of Semiconductor-Organic Monolayers under Ambient Conditions

Organic monolayers on semiconductor surfaces can also be made under ambient conditions via a wide range of methods (shown in **Figure 1*d–f***). In order for the monolayers to form, it is usually necessary to remove oxide layers and passivate the surface against additional reaction. This is typically achieved using simple monatomic reagents to coordinately saturate all surface bonds. The most common passivating agent is hydrogen (68), but other halogens including chlorine (69, 70) and iodine (71) have been used. The goal of the passivation step is to provide all surface atoms with a nearly ideal coordination, thereby reducing their reactivity toward the ambient atmosphere. Hydrogen is a common passivating agent because H-terminated surfaces of silicon exhibit very low densities of mid-gap surface electronic states (68) and because silicon samples, when immersed in a solution of HF or NH_4F, become H-terminated. HF is excellent at removing surface oxides but does not etch the underlying silicon very quickly. NH_4F etches the silicon as well, but is highly anisotropic. Typically, dilute (∼2%–10%) HF is used to passivate the Si(001) surface and ∼40% NH_4F is used on the (111) face (72). Most ambient-condition studies using silicon use the (111) face because the anisotropic nature of the NH_4F leads to a spontaneous smoothing of the Si(111) surface, but leads to roughening of the (001) surface (73–75).

Once the starting surface is obtained, reaction with alkenes and other unsaturated compounds can occur as depicted in **Figure 1*d–f***; however, reactions require some form of activation. The reactions of Si–H bonds with alkenes are often analogous to classical hydrosilylation reactions, in which Lewis acids such as $EtAlCl_2$ are able to enhance the reactions of H-terminated silicon with organic alkenes and alkynes (76, 77).

The reaction of H-terminated surfaces with simple alkenes can be initiated by diacyl peroxides, which decompose when heated to form radicals that can abstract hydrogen atoms from the surface (78, 79), thereby exposing coordinatively unsaturated "dangling bonds." Similarly, Bowden and colleagues used 4-(decanoate)-2,2,6,6-tetramethylpiperidinooxy (TEMPO) as a radical initiator to link unprotected carboxylic acids to the Si(111) surfaces (80). As an alternative to chemical activation, thermal activation has been successfully used, typically by immersing the H-terminated Si surfaces in the alkenes of interest and heating them for extended periods (hours to days) at ∼200°C (72, 78, 79, 81). Recently, there has been great interest in the use of photochemical activation, initiated by UV light at wavelengths of ∼254 nm (82–86). The use of light is an attractive option because it provides a way to pattern

the surfaces with different molecular groups to form molecular arrays. Electrografting can also be used to link alkenes and alkynes to H-terminated Si surfaces, although it appears that there are important mechanistic differences between these (87, 88). These studies have demonstrated that there are multiple ways to achieve the reaction of alkenes with silicon and diamond surfaces.

In addition to alkenes, a number of other functional groups including thiols, alcohols, and aldehydes react directly with the H-terminated surface with suitable activation, forming Si–S–C Si–O–C linkages and/or siloxane esters (89–91). Although most early studies of the functionalization of silicon focused on forming surfaces terminated with alkyl chains, the practical utility of monolayers on silicon often requires the ability to form a molecular layer containing well-defined functional groups at the distal end. In most cases involving two reactive groups, such as a terminal alkene with an alcohol or carboxylic acid group at the distal end, the resulting layers are typically disordered and consist of a mixture of both groups. Consequently, to achieve well-defined functional monolayers it is necessary to identify chemical groups that are unreactive toward the surface during the grafting process, but which can be deprotected after grafting to expose synthetically useful reactive groups (72). The choice of protecting group and deprotection conditions often can be based on known wet-chemical methods (92).

Sieval et al. were the first to successfully demonstrate this approach. They functionalized silicon with olefins bearing ester groups using thermal activation, and showed that they could be reduced to form alcohol-modified surfaces or oxidized to carboxylic acids (72). Boukherroub et al. showed that photochemical reactions with ethyl undecylenate with Si(111) led to ester-modified surfaces that could subsequently be converted to produce carboxylic acid–modified surfaces (93). Strother and colleagues used a similar process to link esters to the surface (83); they showed that by deprotecting the samples and using standard biochemical methods, it was possible to prepare well-defined DNA-modified surfaces exhibiting good selectivity toward binding of complementary versus noncomplementary sequences in solution, as well as good stability.

Whereas H-terminated silicon surfaces are relatively unreactive, Cl-terminated surfaces are more reactive and therefore more amenable to additional methods of modification. Bansal and Lewis (69, 70) formed organic monolayers on Cl-terminated silicon surfaces followed by reactions with Grignard reagents and with organolithium compounds (shown in **Figure 1*f***). Use of this method has yielded layers exhibiting excellent passivation properties (69).

3. CHARACTERIZATION OF ORGANIC MONOLAYERS ON SEMICONDUCTORS

The characterization of organic monolayers typically involves a combination of multiple techniques. For chemical analysis, the most commonly used methods are Fourier transform infrared spectroscopy (FTIR) and X-ray photoelectron spectroscopy (XPS). These techniques complement one another in terms of the types of information they provide. Although the frequencies and intensities of the

vibrational modes observed in FTIR provide detailed information about the nature of the chemical functional groups, FTIR spectra are difficult to relate to absolute numbers of molecules and functional groups because of the absence of reliable standards for surface measurements and because the electromagnetic boundary conditions, quantum-mechanical selection rules, and coupling between molecules at semiconductor interfaces are complicated. XPS provides excellent information about the elements and their oxidation states and is generally more useful than FTIR for quantitative analysis because the selection rules for excitation of core levels are rather straightforward and because standards are readily available.

For spatial information, scanned-probe methods such as scanning tunneling microscopy (STM) provide state-of-the-art spatial resolution, but work well only on very flat surfaces. STM in particular can be applied only to organic layers that are sufficiently conductive for electrons to tunnel through. Recent studies show that scanning electron microscopy (SEM) can provide useful information about molecular layers on submicron length scales; such data are interesting in part because the SEM imaging process involves transmission of low-energy electrons through the layers.

3.1. Scanning Tunneling Microscopy

STM remains one of the primary tools for obtaining direct, atomic-level information about bonding at organic-semiconductor interfaces. Using STM as a tool for surface analysis, several types of information can be obtained, such as the location of molecules on the surface, the number and atomic geometry of different bonding configurations, and the electronic structure of individual adsorbed molecules. However, because STM images represent a convolution of the electronic density of states and the local barrier to electron tunneling, it is often difficult to extract sufficiently quantitative information. Nevertheless, STM is unparalleled in its ability to observe and characterize the structure and electronic properties of individual molecules and molecular layers.

STM has been widely applied to the investigation of molecular layers (15, 16, 18–21, 34, 39, 41, 94). In cases where the molecules are clearly asymmetric in shape, the STM images directly reflect the molecular shape, thereby providing useful information about the bonding locations on the surface. For example, **Figure 2*b*,*c*** shows high-resolution STM images of the molecule 1,5-cyclooctadiene (COD) bonded to the Si(001) surface via a [2+2] cycloaddition reaction (19), yielding an ordered, epitaxial layer of COD molecules. Infrared measurements show that only one C=C bond is involved in bonding, leaving a structure similar to that shown in profile in **Figure 2*a***. In the high-resolution STM images, the ordering of the individual molecules into rows (commensurate with the underlying lattice of Si=Si dimers) can be clearly seen. At the highest resolution (**Figure 2*c***), each molecule is shown to consist of two clear lobes of higher intensity; thus, the STM images can even provide direct information about the intramolecular structure.

At low coverage, the STM is able to provide a measure of the apparent height of individual molecules. The apparent height involves a convolution of geometry and electronic structure, but is of interest for understanding charge transport

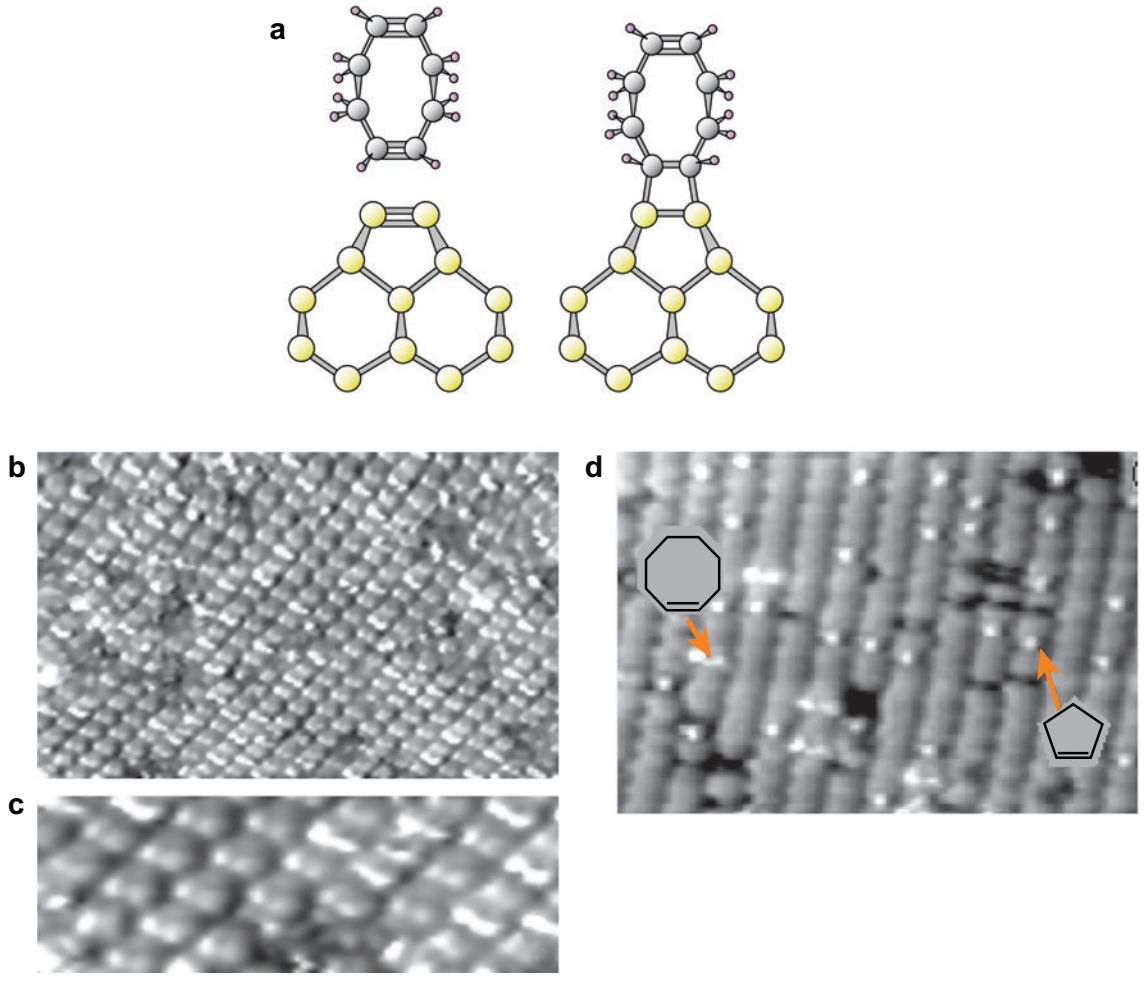

Figure 2

(*a*) Side-view representation of the bonding of 1,5-cyclooctadiene with the Si(001) surface. (*b*, *c*) High-resolution scanning tunneling microscopy (STM) images of the resulting molecular layers. (*d*) High-resolution STM images showing two different molecules, cyclopentene and cyclooctene, bonded to the Si(001) surface. The STM images reveal the locations of bonding with respect to the underlying dimer rows, and also show that the cyclopentene and cyclooctene molecules have different shapes. Reproduced with permission from Reference 41.

through molecules. Images of surfaces containing two different molecules provide information about the relative conductivity of the different molecules. For example, **Figure 2*d*** shows a Si(001) surface that was exposed to a mixture of cyclopentene and cyclooctene (41). The STM image clearly shows molecules with two distinct shapes: Some molecules appear as individual bright spots centered along the rows of underlying Si=Si dimers (which are barely resolved in this image), whereas the others appear

as closely spaced pairs of lobes. By varying the amount of each of the two molecules in the dosing gas, it is easy to identify each molecule in order to confirm their identities. Thus, STM clearly has the ability to distinguish between different molecular species on a surface.

The ability to identify molecules on an a priori basis is also possible in principle. However, the images from the STM reflect a somewhat complex convolution of information about the electronic density of states of the sample and tip, combined with an understanding of the electronic barrier between them (48). Continued interest in understanding charge transport through individual molecules and the fabrication of single-molecule devices (95) has led to further efforts to develop practical theoretical formalisms for predicting the apparent shapes, heights, and other features of molecules as viewed via STM. Much of the original work in the field applied the Tersoff-Hamann theory (96, 97) which is a derivative of the broader Bardeen theory of electron tunneling. In the Tersoff-Hamann theory, the tunneling current is controlled by the density of states and by the probability of electron tunneling, which in turn is controlled primarily by the sample-tip separation and by the local barrier height (work function). However, there are a number of approximations (nearly planar surface, spherical tip) that render this theory inappropriate for understanding images of single molecules, especially on semiconducting surfaces and at higher bias. Ratner and colleagues have been particularly successful using scattering methods incorporating Green's functions (98, 99).

Measurements of the current as a function of the applied voltage, commonly referred to as tunneling spectroscopy (100, 101), can be used to probe the electronic properties of individual molecules (101, 102). This approach has been widely used to characterize the current-voltage characteristics of molecules and molecular layers. Of particular interest has been the observation of negative differential resistance over certain types of molecular structures (103, 104). Tunneling spectroscopy measurements (measurements of current as a function of voltage at specific locations) are complementary to voltage-dependent STM images (measurements of the variation in apparent height at different applied voltages); both provide information on the electrical characteristics as a function of space and applied voltage.

3.2. X-Ray Photoelectron Spectroscopy

XPS is one of the principal methods used to obtain information about the chemical composition of surfaces and monolayers (105). A significant advantage of XPS over almost all other surface analytical methods is that XPS can be performed in a quantitative manner. Detailed analysis of chemical shifts can provide additional insights into the effective oxidation states of surface species. More importantly, the X-ray absorption and photoelectron emission cross sections of core-level transitions are not very sensitive to the local chemical environment; consequently, it is possible to tabulate the relative sensitivity factors for various elements and to use these data to relate the observed intensities to actual concentrations in a relatively straightforward manner.

XPS at low-energy resolution provides an elemental analysis of the surface species. At higher resolution, additional chemical information is obtained through the

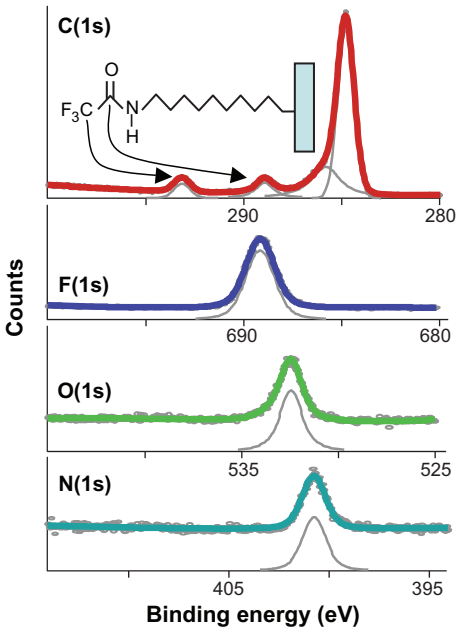

Figure 3

X-ray photoelectron spectroscopy (XPS) spectra of a monolayer of trifluoroacetamide-protected aminodecene covalently bonded to a diamond surface. The different oxidation states of carbon in the $-CF_3$ and carbonyl group can be easily resolved. The sharpness of the peaks for the other elements confirms the chemical homogeneity of the monolayer.

core-level shift. Surface species undergo shifts in their core-level binding energies due to the presence of electron-withdrawing or electron-donating groups. The bonding of electron-withdrawing groups increases the XPS binding energies, typically by ~1–2 eV per unit change in the formal oxidation state. **Figure 3**, for example, shows an XPS spectrum of a monolayer of trifluoroacetamide-protected aminodecene. In this case, bonding of the molecule to the surface leads to at least four distinct types of carbon. The strong electron-withdrawing nature of the F atoms in the CF_3 group increases the binding energy from ~285 eV (characteristic of the alkyl chain and the underlying diamond substrate) to 293 eV, as the formal oxidation state of the C atoms changes from 0 to +3.

The use of quantitative XPS measurements to characterize monolayers on semiconductor surfaces is relatively straightforward. By measuring the ratio of a core-level characteristic of the organic monolayer [such as the C(1s) layer] and another core-level characteristic of the underlying bulk [such as Si(2p)], the number of molecules per unit area can be obtained. The electron escape depths in XPS are typically ~2 nm; this thickness is comparable to that of most molecular monolayers such that the inelastic scattering of the electrons must be accounted for in order to perform quantitative analysis. For a uniform thin film, the electrons from the bulk are attenuated exponentially with distance, so that the integrated intensity of photoemitted

electrons from the bulk is given by:

$$A_B = \int_t^{\infty} \sigma_B \rho_B \exp^{\frac{-(z-t)}{\lambda_{B,B}\sin\theta}} \exp^{\frac{-t}{\lambda_{B,L}\sin\theta}} dz = \sigma_B \rho_B \lambda_{B,B} \sin\theta \exp^{\frac{-t_L}{\lambda_{B,L}\sin\theta}}.$$

The corresponding intensity from the molecular layer is:

$$A_L = \int_0^{t} \sigma_L \rho_L \exp^{\frac{-t}{\lambda_{L,L}\sin\theta}} dz = \sigma_L \lambda_{L,L} \rho_L \sin\theta \left(1 - \exp^{\frac{-t_L}{\lambda_{L,L}\sin\theta}}\right).$$

The observed ratio of intensities is then given by:

$$\frac{A_L}{A_B} = \frac{\rho_L}{\rho_B}\frac{\lambda_{L,L}}{\lambda_{B,B}}\frac{\sigma_L}{\sigma_B}\frac{\left(1 - \exp^{\frac{-t_L}{\lambda_{L,L}\sin\theta}}\right)}{\exp^{\frac{-t_L}{\lambda_{B,L}\sin\theta}}}.$$

In these equations, $\lambda_{B,B}$, $\lambda_{B,L}$, and $\lambda_{L,B}$ are the inelastic mean free paths of electrons of the bulk phase passing through the bulk [i.e., Si(2p) photoelectrons in silicon], electrons of the bulk phase passing through the layer [i.e., Si(2p) photoelectrons in the organic layer], and electrons of the monolayer phase passing through the monolayer [i.e., C(1s) electrons in the organic film], respectively. σ_B and σ_L are the photoelectron cross sections (often represented as sensitivity factors), ρ_B and ρ_L are the volume densities of the bulk and surface, and A_B and A_L are the measured peak areas. Constant factors such as the incident excitation intensity are omitted.

Perhaps the biggest challenge to quantitative analysis via this method is the uncertainty in the effective scattering probability within the organic film. In some cases, the scattering probability has been measured directly by making two samples and directly comparing the intensity of emission of the bulk peaks on the "bare" and functionalized samples (105).

3.3. Valence-Band Photoemission and Inverse Photoemission Electron Spectroscopy

Although XPS provides information about the elemental composition of the sample and effective oxidation state within molecular layers, measurements of valence electronic states are more typically performed using ultraviolet photoemission spectroscopy (UPS), also often referred to as valence-band photoemission. Functionally, this method involves replacing the X-ray source of XPS with a UV excitation source, typically a He-discharge lamp or, for higher resolution and count rates, a synchrotron source. UPS has higher energy resolution than XPS and is better suited to analysis of the valence bands. UPS can very easily determine the position of the valence-band edge with respect to the Fermi energy and can measure the work function. Its complementary technique, inverse photoemission electron spectroscopy (IPES), involves sending an electron of known energy onto the sample and measuring the intensity of emitted photons. IPES yields information about the empty electronic states, such as the semiconductor conduction band and, more importantly, the unfilled states associated with the surface electronic states. **Figure 4*a*** depicts the energy schemes for both UPS and IPES measurements.

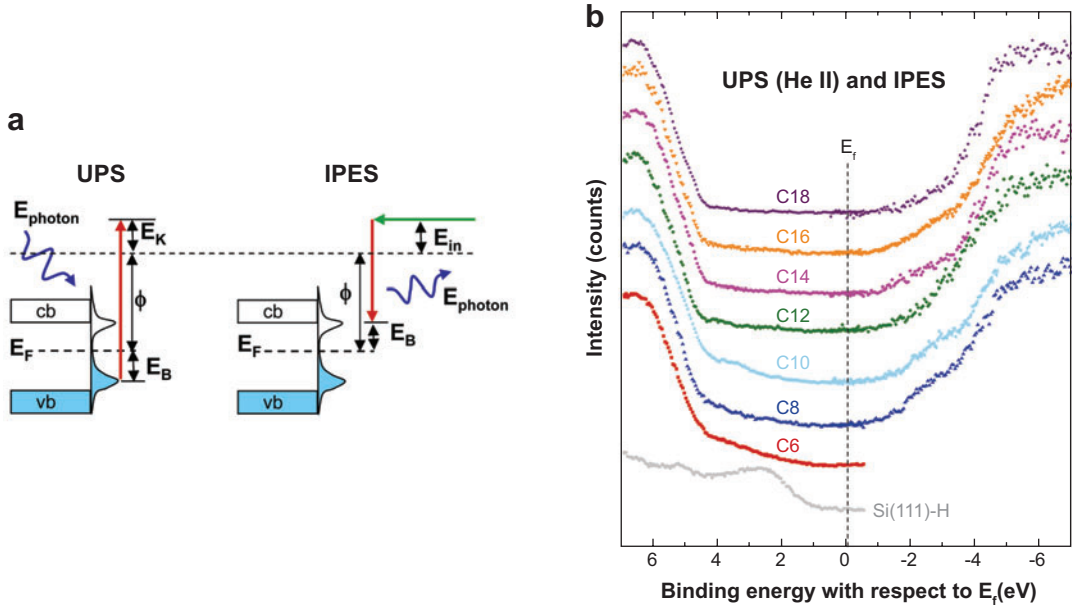

Figure 4

(*a*) Energy level schematic for ultraviolet photoemission spectroscopy (UPS) and inverse photoemission electron spectroscopy (IPES). (*b*) UPS and IPES data for alkyl chains of different lengths bonded to Si(001) surface.

Recent experiments by Segev et al. investigated both the filled and empty valence orbitals and have compared them using theoretical calculations (106). An important consequence of these studies is the first identification of electronic state within the bandgap induced by the interface arising from hybridization of the electronic states of the silicon and the organic layer. **Figure 4*b*** shows UPS and IPES data for monolayers of different lengths; the significant intensity within the bulk bandgap of the semiconductor reveals the presence of new electronic states associated with the Si-C interface. Such states are important in controlling charge transport in molecular systems.

3.4. Infrared Spectroscopy of Organic Monolayers

Infrared spectroscopy has been widely used to characterize the properties of organic monolayers at semiconductor surfaces. Measurements can be performed in a number of experimental geometries, including single-bounce external reflection and multiple internal reflection (MIR) geometries (107). Many aspects of the theory of infrared spectroscopy at surfaces have been reviewed by Chabal (107). One important aspect of infrared spectroscopy at semiconductor surfaces is that the selection rules are quite different from metal surfaces. The boundary conditions are different for s-polarized light (which has the electric field perpendicular to the plane formed by the incident and outgoing beams, and therefore also has the electric field parallel to the surface) and

p-polarized light (which has the electric field in the plane formed by the incident and outgoing beams). For metal surfaces, the electromagnetic boundary conditions cause a cancellation effect for s-polarized light and an enhancement for p-polarized light. Hence, techniques such as polarization-modulation infrared spectroscopy can be used to enhance the sensitivity at metal surfaces and to provide a well-defined background for the infrared spectroscopy measurements. At semiconductor surfaces, however, the dielectric nature of the materials leads to quite distinct selection rules. Because both s- and p-polarized light can interact with molecular species, measurements using polarized light can provide useful information about the orientation of molecules, both along the surface normal and within the sample plane.

Information may be obtained from the frequencies, intensities, and polarization dependences of the spectra. At submonolayer coverages, FTIR is particularly useful for helping to identify molecular bonding configurations. For example, numerous studies have investigated the interaction of organic alkenes with silicon surfaces. Because the C–H stretching modes of alkene are higher than those of saturated alkanes, the presence or absence of the alkene stretch can be used to determine whether or not the molecules bind to the surface via the alkene group (15).

FTIR can also be used to identify molecular orientations on the surface. To gain insight into the azimuthal orientation of molecular functional groups, a substrate with a uniform orientation must be used. The (001) surface of silicon consists of Si=Si dimer units whose orientation rotates by 90° across each atomic step; consequently, most surfaces consist of an equal mixture of dimers in each of two configurations. However, by using a sample that is intentionally miscut by ~4° from the (001) plane toward the <110> direction, it is possible to prepare a single-domain surface on which the Si=Si dimers are aligned with their axes all in the same direction (108). Consequently, any orientation dependence in the interaction between the surface and the organic layer can be templated into the orientation of the molecules; in essence, the surface becomes a way of holding molecules in precise orientations, allowing their spectroscopic properties to be probed by controlling the polarization of light (15). Whereas this technique was first used to investigate the interaction of cyclopentene with the Si(001) surface (15), a particularly dramatic example was obtained through the interaction of acetonitrile (CH_3CN) bonded to the Si(001) surface. In this case the interaction with the Si(001) surface produced a C=N bond oriented parallel to the Si=Si dimers. **Figure 5*b*** shows FTIR spectra measured using s-polarized and p-polarized light; very high strong absorbance for the s-polarized light, but not for p-polarized light, demonstrates that the C=N bond is oriented parallel to the Si=Si dimers. It is interesting to note that in this example, the most intense absorption occurred using s-polarized light, which on metallic substrates undergoes a cancellation at the interface due to the image field induced within the metal. This unexpected result illustrates how different the selection rules at semiconductor surfaces are from those at metal surfaces due to the differences in dielectric response of the substrates.

For longer-chain molecules, information on the tilt angle can be obtained from measurements of the reflectivity using s-polarized and p-polarized light. The angle of the infrared transition dipole α can be obtained from the absorbances of s- and

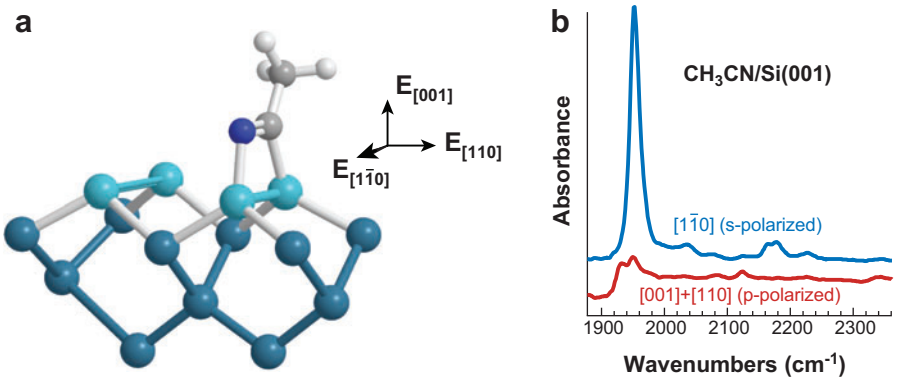

Figure 5

(*a*) Schematic drawing showing the bonding configuration produced by a [2+2] cycloaddition reaction of acetonitrile (CH_3CN) onto the Si(001) surface. (*b*) Polarized Fourier transform infrared spectroscopy (FTIR) data showing a strong absorbance using s-polarized light with the electric field oriented parallel to the C=N bond on the surface.

p-polarized light (A_s and A_p, respectively) via $\alpha_{TD} = \tan^{-1}\sqrt{\left(\frac{2\frac{A_s}{A_p}E_z^2}{E_y^2 - \frac{A_s}{A_p}E_x^2}\right)}$, where E_x, E_y, and E_z represent the magnitude of the electric fields along the x, y, and z directions, respectively (72). These values depend on the index of refraction and the angle of incidence and can be readily calculated using the well-known Fresnel laws. From these measurements, the orientation of the transition dipole for the symmetric (α_a) and antisymmetric (α_{as}) methylene vibrational modes is measured. Once the orientation of these transition dipoles is known, the tilt of the molecules within the layer can be calculated by simple geometry:

$$\phi_{tilt} = 1 - \cos^2 \alpha_s - \cos^2 \alpha_{as}.$$

A third piece of information that can be gleaned from infrared spectra is the degree to which the molecules adopt an all-trans configuration. In pure solid alkenes, all of the molecules in the hydrocarbon chains are in an all-trans configuration such that the carbon backbone of each molecule lies in a single plane. However, in liquid form there is substantial twisting about the individual bonds; these out-of-plane twists, or "gauche defects," alter the frequencies of the methylene ($-CH_2-$) vibrational modes. The infrared vibrational properties have been extensively studied for a variety of alkanethiols on gold (109–111). On gold surfaces, the alkyl chains of self-assembled monolayers give rise to asymmetric and symmetric C–H stretching modes near 2920 cm^{-1} and 2850 cm^{-1}. However, local structural information is contained in subtle shifts from these values, with the $-CH_2-$ asymmetric stretching mode shifting from 2924 cm^{-1} to 2918 cm^{-1} and the symmetric stretching mode shifting from 2855 cm^{-1} to 2851 cm^{-1} when going from liquid-like to solid state (111). Similar ideas have been applied to monolayers grafted onto semiconductor surfaces. Experimental data from photochemical grafting of 1-octene to silicon yielded C–H modes

with frequencies as low as 2920 cm^{-1}, and 1-octadecene yielded 2917 cm^{-1} (85), which is identical (within experimental error) to the frequency of a pure solid alkane. Perring and colleagues showed that undecylenic acid yields 2923 cm^{-1} and 2853 cm^{-1} (80); according to Wang et al., photochemically activated grafting of 1-dodecene to polycrystalline diamond yielded frequencies of 2922 cm^{-1} and 2850 cm^{-1} (112).

3.5. Scanning Electron Microscopy of Monolayers

Although SEM is commonly used as a structural analysis tool, it can also be used to directly image molecular layers on semiconductor surfaces (80, 112–114). This ability stems from the fact that molecular layers alter the potential barriers that commonly exist at surfaces and therefore can significantly impact the yield of secondary electrons. The use of SEM to image the spatial distribution of molecules can also provide important insights into the mechanisms of reactions.

One important question revolves around the nature of contrast in SEM images of molecular monolayers. Early studies of monolayers on gold (115, 116) showed clear contrast between different layers, but in those studies the possible influence of electron beam damage and the presence of surface contamination layers made it difficult to identify the origins of contrast. Studies of thicker layers produced by proteins (117, 118) showed that the contrast was dominated by the scattering of electrons within the molecular layers and was correlated with the mass coverage. On gold, the secondary electrons are essentially all generated within the gold, and the organic layers basically act as an inelastic scattering layer. SEM imaging of patterned molecular layers on semiconductor surfaces has been demonstrated using silicon (80, 119), diamond (112, 120, 121), and gallium nitride (122).

With regard to semiconductors, Saito et al. (113) investigated the contrast among alkoxysilanes with different terminal groups after bonding to oxidized silicon surfaces and found that the contrast among different molecules was determined primarily by the electron affinity of the molecules involved, as calculated via computational chemistry methods. Based on this, the authors proposed that the emission of secondary electrons occurred by excitation from bulk states to normally unoccupied energy levels, followed by excitation into vacuum; consequently, the lowest unoccupied molecular orbital (LUMO) levels closer to the vacuum level (higher in energy) were more effective at enhancing secondary electron yield compared with lower-lying levels.

Recent studies of molecular layers on diamond surfaces have shown a similar trend (112). One particularly interesting aspect of the work on diamond is that contrast is also developed between the H-terminated diamond surface and monolayers of simple hydrocarbons. **Figure 6** shows an SEM image of a diamond sample that was produced using photochemical grafting with a mask in order to produce a central region functionalized with 1-dodecene, whereas the surrounding region consisted of H-terminated diamond. The 1-dodecene monolayer significantly decreased the secondary electron emission. H-terminated diamond has negative electron affinity (i.e., the conduction band is higher in energy than the vacuum level) and is therefore a facile electron emitter; however, pure hydrocarbons also have negative electron affinity. Why, then, does 1-dodecene reduce the electron yield from H-terminated

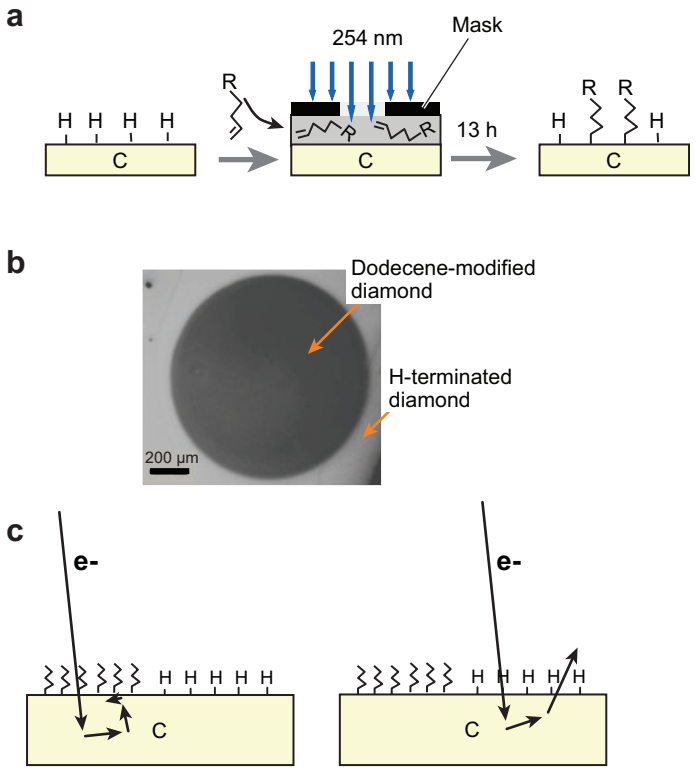

Figure 6

(*a*) Photopatterning of a molecular layer using a simple shadow mask. (*b*) Scanning electron microscopy (SEM) image demonstrating its ability to discriminate functionalized from nonfunctionalized regions. (*c*) Likely mechanism of image contrast, based on electron scattering at the diamond-molecule interface.

diamond? It is likely that the answer lies in treating the electron as a wave. Studies of binary monolayers on gold surface have shown that disorganized layers formed by mixing two different molecules on the surface give rise to lower electron emission than well-ordered layers of either molecule in pure form (123, 124). On diamond and other semiconductor surfaces, most molecular layers are disordered near the semiconductor-molecule boundary as most molecules cannot pack closely enough together to bind to each surface site. The resulting disorder at the semiconductor-organic interface leads to increased scattering electrons at the interface, reducing the secondary electron yield.

3.6. X-Ray Reflectivity and Grazing Incidence X-Ray Diffraction

X-ray methods can be used to probe the variations in electron density perpendicular to and parallel to the interface. By measuring reflectivity as a function of the momentum transfer vector, it is possible to quantify properties such as the density and thickness of the monolayer, the molecular tilt, and interfacial roughness (125). Tidswell et al. (125) developed much of the methodology for analyzing the properties of organic thin films, having obtained their initial data from alkoxysilane monolayers on oxidized silicon surfaces.

More recent experiments have characterized a variety of organic monolayers on semiconductor surfaces. In specular reflectivity measurements, the reflectivity is measured as a function of the momentum transfer vector $Q(\theta) = \frac{4\pi}{\lambda}\sin(\theta)$. For very small values of momentum transfer, total reflection is observed. At high values of momentum transfer, the reflectivity follows the Fresnel laws corresponding to reflection from a single sharp interface. At intermediate values, however, the reflectivity depends on the profile of electron density perpendicular to the surface. By fitting the data, information about the thickness of the film, roughness of the semiconductor-organic interface, and electron density profile can be obtained. The minima in the X-ray reflectivity measurements correspond to $Q = \frac{(2n+1)\pi}{L}$, such that the thickness corresponds to half-integral multiples of the wavelength; consequently, measuring the position and depth of these minima provides a rapid means of identifying the thickness and average density of the molecular layers. Sieval and colleagues examined molecular layers produced by thermal grafting of monolayers to H-terminated Si(100) and Si(111) surfaces and succeeded in determining the thickness of the layers (72, 81). Knowledge of the molecular structure and bond lengths of the alkyl chain was sufficient to determine that the organic layers were tilted with respect to the surface normal by 27°, which is in remarkable agreement with measurements based on the dichroic ratio in infrared spectroscopy. Hersam and colleagues similarly characterized the thickness of 4-bromostyrene monolayers formed on Si(111) surfaces (126).

Whereas X-ray reflectivity measurements typically provide information about the electron density perpendicular to the surface, there is a critical angle below which X-rays undergo total reflection. At these very low angles (on the order of 0.2° or less), the reflectivity provides information about the in-plane ordering. Early studies of monolayers produced by reaction of alkoxysilanes on oxidized silicon showed clear diffraction peaks due to local ordering of the molecular chains. Studies of alkenes ranging from dodecene (C10) to octadecene (C18) showed that the molecular layers are amorphous regardless of length (127). It is noteworthy that although FTIR frequencies and grazing incidence X-ray diffraction (GIXD) data both probe the structural order within a film, the FTIR measurements infer disorder from the presence of gauche defects, whereas GIXD directly probes the spatial periodicity of the surface electron density. Thus, a layer that appears crystalline by FTIR may not necessarily appear ordered by X-ray reflectivity.

3.7. Biomolecular Recognition at Bio-Functionalized Semiconductor Surfaces

Although most studies have focused on single monolayers, more recent studies have addressed many issues associated with the fabrication of organic films for biological applications, especially the use of bio-modified semiconductors for applications such as electronic sensing systems. Early work in this field was targeted toward chemical modification of the silicon oxide surface (5, 128, 129). Wagner et al. conducted early studies of biologically active monolayers linked to monolayers on silicon (130). Strother et al. used photochemical grafting of protected alkenes to single-crystal

Si(001) and Si(111) surfaces via two routes. One route consisted of grafting of alkenyl esters followed by deprotection and conversion to an amine-terminated surface (83), and the second consisted of an alkene with a protected amine group that was subsequently deprotected and linked to DNA. Subsequent deprotection exposed the reactive carboxylic acid and amine groups that were then covalently linked to DNA oligonucleotides (83). More recent studies have shown that other semiconductors, including GaN(123) and diamond (131–134), can be modified via the same route. For biologically modified semiconductors, the primary measures of interest are typically the selectivity of binding (i.e., the degree to which a bio-modified surface will recognize and bind to a complementary target molecule, while rejecting others), the stability of the interfaces, and the electronic properties of the resulting interface. Early studies on silicon usually modified the silicon oxide (5), but the inherent instability of SiO_2 in aqueous solutions and the presence of charged OH^- groups at the surface led to poor sensitivity and poor stability. Organic monolayers bonded directly to Si improve the stability because the organic monolayers act as a hydrophobic barrier layer that prevents water, OH–, and other reactive species from penetrating to the silicon-organic interface. However, even with the protective layers degradation still occurs, which continues to fuel interest in alternative materials such as diamond. Studies by Yang et al. showed that the photochemical functionalization of diamond with organic monolayers, followed by subsequent chemical modification steps, yielded DNA-modified surfaces exhibiting stability superior to that of functionalized silicon, gold, and SiO_2 (134). Stability was also demonstrated at temperatures of 60°C (135), above the DNA-denaturing temperature. A primary motivating factor for biological functionalization of semiconductors is the opportunity to take advantage of the electronic properties of semiconductors for hybrid bio-electronic sensing devices. The case of diamond, however, is even more interesting because the extreme hardness of diamond makes it useful in applications such as biomedical implants, where mechanical properties as well as biological response may be important to achieve long-term functionality.

Using organic monolayers as interfaces between semiconductors and biomolecules, several groups have demonstrated the ability to achieve direct detection of biomolecules such as DNA (4, 136, 137) and antibodies (131, 133). In such studies, the binding of DNA is typically measured in two ways. The first is to link one strand of DNA to the surface and to measure the intensity of fluorescence from the surface after exposure to molecules having a complementary sequence with a fluorescent tag. The second is to investigate the changes in electrical response. The ability to directly detect biological binding processes arises from the fact that binding of charged biomolecules near the semiconductor surface changes the electrostatic potential, which in turn leads to a change in the band-bending and the associated conductivity near the surface of the semiconductor. This change in conductivity can be measured in two ways. One way is to measure the electrical impedance between the modified semiconductor surface and a counter-electrode in solution, usually using a three-electrode potentiostat. Studies have been performed on silicon (4, 136, 137) and diamond (132, 133) surfaces. These studies showed that at frequencies between ~1 kHz and ~1 MHz, the impedance of the system was dominated by the impedance

of the semiconductor space-charge layer; consequently, binding of molecules to the surface altered the resistance and capacitance of the space-charge layer, producing a significant change in the overall impedance of the system. This impedance measurement has been used to detect antibody-antigen binding (133). The second method of characterizing the electrical response is to use a field-effect transistor geometry, in which one deposits two metallic contacts (the source and drain of the transistor) onto the surface and then measures the change in current parallel to the surface (131).

Fundamentally, electrochemical impedance spectroscopy (EIS) and the field effect transistor (FET) both measure the semiconductor space-charge layers but differ as to whether the impedance is measured perpendicular to (EIS) or parallel to (FET) the interface. The EIS geometry does not require any special fabrication techniques, but in order to be sensitive to the semiconductor space-charge region it is necessary to operate at the correct frequency. The FET geometry requires special fabrication techniques but can be performed at any frequency, including dc.

For many biological applications, the ability to control the selectivity of binding, especially to eliminate the nonspecific binding of proteins and other biomolecules, is critical. Early studies of self-assembled monolayers on gold showed that ethylene glycol oligomers were very effective at restricting the nonspecific binding of many proteins. Lasseter and colleagues (139) grafted alkenes bearing ethylene glycol groups to surfaces of silicon, diamond, and gold; a quantitative comparison showed that functionalized diamond and gold surfaces were comparable to or possibly even better than those reported previously on modified gold surfaces (138, 139). Lasseter et al. also demonstrated that by making mixed monolayers consisting of ethylene glycol groups with interspersed attachment points covalently linked to biotin, it was possible to detect the complementary protein avidin in undiluted serum with only minimal interference (139).

3.8. Electronic Properties of Molecules at Semiconductor Surfaces

Understanding the electrical properties of molecules at surfaces is crucial for a number of emerging applications, including molecular electronics and the use of semiconductors as a basis for chemical and biological sensing. A variety of classical and nonclassical electrochemical measurements have been used to characterize the properties of organic monolayers (69, 70, 140–146). Impedance measurements, in which the interfacial impedance is measured as a function of frequency, are especially useful as a means to determine the resistance and capacitance of organic monolayers and their interfaces. The most common method, EIS, uses a small ac potential to characterize the small-signal response as a function of frequency and dc potential, typically performed in electrolyte solution using a three-electrode potentiostat (147). EIS measurements are useful because the electronic properties of semiconductor-organic interfaces typically contain contributions from the resistance and capacitance of the semiconductor space-charge region, the capacitance and electron-transfer resistance of the monolayer, and the capacitance of the electrochemical double layer.

By measuring the response over a wide range of frequencies and fitting it to circuit models, it is possible to extract the values of the individual components (137). Two

parameters of particular interest have been the capacitance and resistance of the organic monolayers. Bansal et al. found that alkyl monolayers on silicon have excellent passivation properties against electrochemical oxidation (69, 70). The possibility of using organic monolayers as a dielectric has led to interest in characterizing the capacitance of individual monolayers and organosilane monolayers electrochemically grafted to silicon surfaces (147, 148). Yu et al. investigated organic monolayers and found that they formed molecular capacitors on Si with a dielectric constant of approximately 3.3. By adding a known quantity of a redox agent such as dimethylferrocene, it is possible to quantitatively evaluate the extent to which an organic monolayer blocks electron-transfer reactions (69).

4. SUMMARY

The use of organic monolayers provides a unique opportunity to achieve improved integration of semiconductors with organic and biological molecules. Continued advances in the synthesis and characterization of these layers will further expand the range of possible applications of molecular monolayers as interfaces between semiconductors and a wider range of organic and/or biological materials.

DISCLOSURE STATEMENT

The author is not aware of any biases that might be perceived as affecting the objectivity of this review.

ACKNOWLEDGMENTS

This work is based in part on research funded by the National Science Foundation, grant nos. CHE-0613010 and DMR-0425880.

LITERATURE CITED

1. Allara DL. 1995. Critical issues in applications of self-assembled monolayers. *Biosens. Bioelectron.* 10:771–83
2. Mirkin CA, Ratner MA. 1992. Molecular electronics. *Annu. Rev. Phys. Chem.* 43:719–54
3. Aviram A, Ratner MA. 1974. Molecular rectifiers. *Chem. Phys. Lett.* 29:277–83
4. Fritz J, Cooper EB, Gaudet S, Sorger PK, Manalis SR. 2002. Electronic detection of DNA by its intrinsic molecular charge. *Proc. Nat. Acad. Sci. USA* 99:14142–46
5. Bergveld P. 1996. The future of biosensors. *Sens. Actuators A.* 56:65–73
6. Appelbaum JA, Baraff GA, Hamann DR. 1976. The Si(100) surface. III. Surface reconstruction. *Phys. Rev. B* 14:588–601
7. Appelbaum JA, Hamann DR. 1976. Electronic structure of solid surfaces. *Rev. Mod. Phys.* 48:479–96

8. Hamers RJ, Tromp RM, Demuth JE. 1986. Scanning tunneling microscopy of Si(001). *Phys. Rev. B* 34:5343–57
9. Buriak JM. 2001. Diamond surfaces: just big organic molecules? *Angew. Chem. Int. Ed.* 40:532–34
10. Liu H, Hamers RJ. 1997. Stereoselectivity in molecule-surface reactions: adsorption of ethylene on silicon(001) surfaces. *J. Am. Chem. Soc.* 119:7593–94
11. Coulter SK, Hovis JS, Ellison MD, Hamers RJ. 2000. Reactions of substituted aromatic hydrocarbons with the Si(001) surface. *J. Vac. Sci. Tech. A* 18:1965–70
12. Ellison MD, Hamers RJ. 1999. Adsorption of phenyl isothiocyanate on Si(001): a 1,2-dipolar surface addition reaction. *J. Phys. Chem. B* 103:6243–51
13. Hamers RJ, Butler JE, Lasseter T, Nichols BM, Russell JN, et al. 2005. Molecular and biomolecular monolayers on diamond as an interface to biology. *Diamond Relat. Mater.* 14:661–68
14. Hamers RJ, Coulter SK, Ellison MD, Hovis JS, Padowitz DF, et al. 2000. Cycloaddition chemistry of organic molecules with semiconductor surfaces. *Acct. Chem. Res.* 33:617–24
15. Hamers RJ, Hovis J, Lee S, Liu H, Shan J. 1997. Formation of ordered, anisotropic organic monolayers on the Si(001) surface. *J. Phys. Chem.* 101:1489–92
16. Hovis J, Lee S, Liu H, Hamers RJ. 1997. Controlled formation of organic layers on semiconductor surfaces. *J. Vac. Sci. Technol. B* 15(4):1153–58
17. Hovis JS, Coulter SK, Hamers RJ, D'Evelyn MP, Russell JN, Butler JE. 2000. Cycloaddition chemistry at surfaces: reaction of alkenes with the diamond(001)–2 × 1 surface. *J. Am. Chem. Soc.* 122:732–33
18. Hovis JS, Hamers RJ. 1998. Structure and bonding of ordered organic monolayers of 1,3,5,7-cyclooctatetraene on the Si(001) surface: surface cycloaddition chemistry of an antiaromatic molecule. *J. Phys. Chem. B* 102:687–92
19. Hovis JS, Hamers RJ. 1997. Structure and bonding of ordered organic monolayers of 1,5-cyclooctadiene on the silicon(001) surface. *J. Phys. Chem. B* 101:9581–85
20. Hovis JS, Liu H, Hamers RJ. 1998. Cycloaddition chemistry and formation of ordered organic monolayers on silicon(001) surfaces. *Surf. Sci.* 402–404:1–7
21. Hovis JS, Liu HB, Hamers RJ. 1998. Cycloaddition chemistry of 1,3-dienes on the silicon(001) surface: competition between [4+2] and [2+2] reactions. *J. Phys. Chem. B* 102:6873–79
22. Konecny R, Doren DJ. 1998. Cycloaddition reactions of unsaturated hydrocarbons on the Si(100)–2 × 1 surface: theoretical predictions. *Surf. Sci.* 417:169–88
23. Teplyakov AV, Kong MJ, Bent SF. 1997. Vibrational spectroscopic studies of Diels-Alder reactions with the Si(100)–2 × 1 surface as a dienophile. *J. Am. Chem. Soc.* 119:11100–1
24. Teplyakov AV, Kong MJ, Bent SF. 1998. Diels-Alder reactions of butadienes with the Si(100)–2 × 1 surface as a dienophile: vibrational spectroscopy, thermal desorption and near edge X-ray adsorption fine structure studies. *J. Chem. Phys.* 108:4599–606
25. Wang GT, Bent SF, Russell JN, Butler JE, D'Evelyn MP. 2000. Functionalization of diamond(100) by Diels-Alder chemistry. *J. Am. Chem. Soc.* 122:744–45

26. Bent SF. 2002. Organic functionalization of group IV semiconductor surfaces: principles, examples, applications, and prospects. *Surf. Sci.* 500:879–903
27. Russell JN, Butler JE, Wang GT, Bent SF, Hovis JS, et al. 2001. Pi-bond vs radical character of the diamond(100)–2 × 1 Surface. *Mat. Chem. Phys.* 72:147–51
28. Filler MA, Bent SF. 2003. The surface as molecular reagent: organic chemistry at the semiconductor interface. *Prog. Surf. Sci.* 73:1–56
29. Filler MA, Mui C, Musgrave CB, Bent SF. 2003. Competition and selectivity in the reaction of nitriles on Ge(100)–2 × 1. *J. Am. Chem. Soc.* 125:4928–36
30. Choi CH, Gordon MS. 1999. Cycloaddition reactions of 1,3-cyclohexadiene on the silicon(001) surface. *J. Am. Chem. Soc.* 121:11311–17
31. Schwartz MP, Hamers RJ. 2007. Reaction of acetonitrile with the silicon(001) surface: a combined XPS and FTIR study. *Surf. Sci.* 601:945–53
32. Schwartz MP, Hamers RJ. 2002. The role of pi-conjugation in attachment of organic molecules to the silicon(001) surface. *Surf. Sci.* 515:75–86
33. Schwartz MP, Halter RJ, McMahon RJ, Hamers RJ. 2003. Formation of an atomically abrupt interface between a polycyclic aromatic molecule and the silicon(001) surface via direct Si-C linkage. *J. Phys. Chem. B* 107:224–28
34. Schwartz MP, Ellison MD, Coulter SK, Hovis JS, Hamers RJ. 2000. Interaction of pi-conjugated organic molecules with pi-bonded semiconductor surfaces: structure, selectivity, and mechanistic implications. *J. Am. Chem. Soc.* 122:8529–38
35. Schwartz MP, Barlow DE, Weidkamp KP, Russell JN, Butler J, et al. 2006. 1,3-H-transfer for CHD on Si(001). *J. Am. Chem. Soc.* 128:11054–61
36. Schwartz MP, Barlow DE, Russell JN, Weidkamp KP, Butler JE, et al. 2006. Semiconductor surface-induced 1,3-hydrogen shift: the role of covalent vs Zwitterionic character. *J. Am. Chem. Soc.* 128:11054–61
37. Schwartz MP, Barlow DE, Russell JN, Butler JE, D'Evelyn MP, Hamers RJ. 2005. Adsorption of acrylonitrile on diamond and silicon(001)–(2 × 1) surfaces: effects of dimer structure on reaction pathways and product distributions. *J. Am. Chem. Soc.* 127:8348–54
38. Fang LA, Liu JM, Coulter S, Cao XP, Schwartz MP, et al. 2002. Formation of pi-conjugated molecular arrays on silicon(001) surfaces by heteroatomic Diels-Alder chemistry. *Surf. Sci.* 514:362–75
39. Lee SW, Hovis JS, Coulter SK, Hamers RJ, Greenlief CM. 2000. Cycloaddition chemistry on germanium(001) surfaces: the adsorption and reaction of cyclopentene and cyclohexene. *Surf. Sci.* 462:6–18
40. Konecny R, Doren DJ. 1997. Theoretical prediction of a facile Diels-Alder reaction on the Si(100)–2 × 1 surface. *J. Am. Chem. Soc.* 119:11098–99
41. Padowitz DF, Hamers RJ. 1998. Voltage-dependent STM images of covalently bound molecules on Si(100). *J. Phys. Chem. B* 102:8541–45
42. Woodward RB, Hoffmann R. 1970. *The Conservation of Orbital Symmetry*. New York: Academia
43. Lee SW, Nelen LN, Ihm H, Scoggins T, Greenlief CM. 1998. Reactions of 1,3-cyclohexadiene with the Ge(100) surface. *Surf. Sci.* 410:L773–78

44. Choi CH, Gordon MS. 2002. Cycloaddition reactions of acrylonitrile on the Si(001) Surface. *J. Am. Chem. Soc.* 124:6162–67
45. Fitzgerald DR, Doren DJ. 2000. Functionalization of diamond(100) by cycloaddition of butadiene: first-principles theory. *J. Am. Chem. Soc.* 122:12334–39
46. Hossain MZ, Aruga T, Takagi N, Tsuno T, Fujimori N, et al. 1999. Diels-Alder reaction on the clean diamond(100)–2 × 1 surface. *J. Appl. Phys. Pt. 2 Lett.* 38:L1496–98
47. Barriocanal JA, Doren DJ. 2001. Cycloaddition of carbonyl compounds on Si(100): new mechanisms and approaches to selectivity for surface cycloaddition reactions. *J. Am. Chem. Soc.* 123:7340–46
48. Hofer WA, Fisher AJ, Lopinski GP, Wolkow RA. 2001. Adsorption of benzene on Si(100)–(2 × 1): adsorption energies and STM image analysis by ab initio methods. *Phys. Rev. B* 63:085314
49. Jung YS, Gordon MS. 2005. Cycloaddition of benzene on Si(100) and its surface conversions. *J. Am. Chem. Soc.* 127:3131–39
50. Lee JY, Cho JH. 2005. Conversion between two binding states of benzene on Si(001). *Phys. Rev. B* 72:235317
51. Shimomura M, Munakata M, Honma K, Widstrand SM, Johansson L, et al. 2003. Structural study of benzene adsorbed on Si(001) surface by photoelectron diffraction. *Surf. Rev. Lett.* 10:499–503
52. Qu YQ, Han KL. 2004. Theoretical studies of benzonitrile at the Si(100)–2 × 1 surface. *J. Phys. Chem. B* 108:8305–10
53. Tao F, Wang ZH, Chen XF, Xu GQ. 2002. Selective attachment of benzonitrile on Si(111)–7 × 7: configuration, selectivity, and mechanism. *Phys. Rev. B* 65:115311
54. Takeuchi N, Selloni A. 2005. Density functional theory study of one-dimensional growth of styrene on the hydrogen-terminated Si(001)–(3 × 1) surface. *J. Phys. Chem. B* 109:11967–72
55. Coulter SK, Schwartz MP, Hamers RJ. 2001. Sulfur atoms as tethers for selective attachment of aromatic molecules to silicon(001) surfaces. *J. Phys. Chem. B* 105:3079–87
56. Bermudez VM. 2002. Functionalizing the GaN(0001)–(1 × 1) surface I. The chemisorption of aniline. *Surf. Sci.* 499:109–23
57. Yamamoto H, Butera RA, Gu Y, Waldeck DH. 1999. Characterization of the surface to thiol bonding in self-assembled monolayer films of $C_{12}H_{25}SH$ on InP(100) by angle-resolved X-ray photoelectron spectroscopy. *Langmuir* 15:8640–44
58. Lim H, Carraro C, Maboudian R, Pruessner MW, Ghodssi R. 2004. Chemical and thermal stability of alkanethiol and sulfur passivated InP(100). *Langmuir* 20:743–47
59. Jun Y, Zhu XY, Hsu JWP. 2006. Formation of alkanethiol and alkanedithiol monolayers on GaAs(001). *Langmuir* 22:3627–32
60. Lunt SR, Santangelo PG, Lewis NS. 1991. Passivation of GaAs surface recombination with organic thiols. *J. Vac. Sci. Tech. B* 9:2333–36

61. Hou T, Greenlief M, Keller SW, Nelen L, Kauffman JF. 1997. Passivation of GaAs(100) with an adhesion promoting self-assembled monolayer. *Chem. Mater.* 9:3181–86
62. Gu Y, Waldeck DH. 1998. Electron tunneling at the semiconductor-insulator-electrolyte interface: photocurrent studies of the n-InP-alkanethiol-ferrocyanide system. *J. Phys. Chem. B* 102:9015–28
63. Casaletto MP, Carbone M, Piancastelli MN, Horn K, Weiss K, Zanoni R. 2005. A high resolution photoemission study of phenol adsorption on Si(100)–2 × 1. *Surf. Sci.* 582:42–48
64. Rummel RM, Ziegler C. 1998. Room temperature adsorption of aniline (C6H5NH2) on Si(100)(2 × 1) observed with scanning tunneling microscopy. *Surf. Sci.* 418:303–13
65. Cao XP, Coulter SK, Ellison MD, Liu HB, Liu JM, Hamers RJ. 2001. Bonding of nitrogen-containing organic molecules to the silicon(001) surface: the role of aromaticity. *J. Phys. Chem. B* 105:3759–68
66. Lopinski GP, Wayner DDM, Wolkow RA. 2000. Self-directed growth of molecular nanostructures on silicon. *Nature* 406:48–51
67. Lu X, Wang XL, Yuan QH, Zhang Q. 2003. Diradical mechanisms for the cycloaddition reactions of 1,3-butadiene, benzene, thiophene, ethylene, and acetylene on a Si(111)–7 × 7 surface. *J. Am. Chem. Soc.* 125:7923–29
68. Yablonovitch E, Allara DL, Chang CC, Gmitter T, Bright TB. 1986. Unusually low surface-recombination velocity on silicon and germanium surfaces. *Phys. Rev. Lett.* 57:249–52
69. Bansal A, Lewis NS. 1998. Electrochemical properties of (111)-oriented n-Si surfaces derivatized with covalently attached alkyl chains. *J. Phys. Chem. B* 102:1067–70
70. Bansal A, Li XL, Lauermann I, Lewis NS, Yi SI, Weinberg WH. 1996. Alkylation of Si surfaces using a two-step halogenation Grignard route. *J. Am. Chem. Soc.* 118:7225–26
71. Cai W, Lin Z, Strother T, Smith LM, Hamers RJ. 2002. Chemical modification and patterning of iodine-terminated silicon surfaces using visible light. *J. Phys. Chem. B* 106:2656–64
72. Sieval AB, Demirel AL, Nissink JWM, Linford MR, van der Maas JH, et al. 1998. Highly stable Si-C linked functionalized monolayers on the silicon (100) surface. *Langmuir* 14:1759–68
73. Higashi GS, Becker RS, Chabal YJ, Becker AJ. 1991. Comparison of Si(111) surfaces prepared using aqueous solutions of NH_4F versus HF. *Appl. Phys. Lett.* 58:1656–58
74. Dumas P, Chabal YJ, Gunther R, Ibrahimi AT, Petroff Y. 1995. Vibrational characterization and electronic properties of long range–ordered, ideally hydrogen-terminated Si(111). *Prog. Surf. Sci.* 48:313–24
75. Dumas P, Chabal YJ. 1991. Electron–energy loss characterization of the H-terminated Si(111) and Si(100) surfaces obtained by etching in NH_4F. *Chem. Phys. Lett.* 181:537–43
76. Buriak JM, Allen MJ. 1998. Lewis acid mediated functionalization of porous silicon with substituted alkenes and alkynes. *J. Am. Chem. Soc.* 120:1339–40

77. Buriak JM, Stewart MP, Geders TW, Allen MJ, Choi HC, et al. 1999. Lewis acid mediated hydrosilylation on porous silicon surfaces. *J. Am. Chem. Soc.* 121:11491–502
78. Linford MR, Chidsey CED. 1993. Alkyl monolayers covalently bonded to silicon surfaces. *J. Am. Chem. Soc.* 115:12631–32
79. Linford MR, Fenter P, Eisenberger PM, Chidsey CED. 1995. Alkyl monolayers on silicon prepared from 1-alkenes and hydrogen-terminated silicon. *J. Am. Chem. Soc.* 117:3145–55
80. Perring M, Dutta S, Arafat S, Mitchell M, Kenis PJA, Bowden NB. 2005. Simple methods for the direct assembly, functionalization, and patterning of acid-terminated monolayers on Si(111). *Langmuir* 21:10537–44
81. Sieval AB, Linke R, Zuilhof H, Sudholter EJR. 2000. High-quality alkyl monolayers on silicon surfaces. *Adv. Mater.* 12:1457–60
82. Effenberger F, Gotz G, Bidlingmaier B, Wezstein M. 1998. Photoactivated preparation and patterning of self-assembled monolayers with 1-alkenes and aldehydes on silicon hydride surfaces. *Angew. Chem. Int. Ed.* 37:2462–64
83. Strother T, Cai W, Zhao XS, Hamers RJ, Smith LM. 2000. Synthesis and characterization of DNA-modified silicon (111) surfaces. *J. Am. Chem. Soc.* 122:1205–09
84. Strother T, Hamers RJ, Smith LM. 2000. Covalent attachment of oligodeoxyribonucleotides to amine-modified Si(001) surfaces. *Nucleic Acids Res.* 28:3535–41
85. Cicero RL, Linford MR, Chidsey CED. 2000. Photoreactivity of unsaturated compounds with hydrogen-terminated silicon(111). *Langmuir* 16:5688–95
86. Stewart MP, Buriak JM. 2001. Exciton-mediated hydrosilylation on photoluminescent nanocrystalline silicon. *J. Am. Chem. Soc.* 123:7821–30
87. Robins EG, Stewart MP, Buriak JM. 1999. Anodic and cathodic electrografting of alkynes on porous silicon. *Chem. Comm.* 2479–80
88. Wang D, Buriak JM. 2005. Electrochemically driven organic monolayer formation on silicon surfaces using alkylammonium and alkylphosphonium reagents. *Surf. Sci.* 590:154–61
89. Cleland G, Horrocks BR, Houlton A. 1995. Direct functionalization of silicon via the self-assembly of alcohols. *J. Chem. Soc. Faraday Trans.* 91:4001–3
90. Boukherroub R, Morin S, Bensebaa F, Wayner DDM. 1999. New synthetic routes to alkyl monolayers on the Si(111) surface. *Langmuir* 15:3831–35
91. Boukherroub R, Morin S, Sharpe P, Wayner DDM, Allongue P. 2000. Insights into the formation mechanisms of Si-OR monolayers from the thermal reactions of alcohols and aldehydes with Si(111)-H. *Langmuir* 16:7429–34
92. Wuts PGM, Greene TW, eds. 2006. *Protective Groups in Organic Synthesis*. New York: Wiley
93. Boukherroub R, Wayner DDM. 1999. Controlled functionalization and multistep chemical manipulation of covalently modified Si(111) surfaces. *J. Am. Chem. Soc.* 121:11513–15
94. Hamers RJ, Hovis JS, Greenlief CM, Padowitz DF. 1999. Scanning tunneling microscopy of organic molecules and monolayers on silicon and germanium (001) surfaces. *Jpn. J. Appl. Phys.* 38:3879–87

95. McCreery RL. 2004. Molecular electronic junctions. *Chem. Mater.* 16:4477–96
96. Tersoff J, Hamann DR. 1983. Theory and application for the scanning tunneling microscope. *Phys. Rev. Lett.* 50:1998–2001
97. Tersoff J, Hamann DR. 1985. Theory of the scanning tunneling microscope. *Phys. Rev. B* 31:805–13
98. Mujica V, Kemp M, Ratner MA. 1994. Electron conduction in molecular wires. 2. Application to scanning tunneling microscopy. *J. Chem. Phys.* 101:6856–64
99. Mujica V, Kemp M, Ratner MA. 1994. Electron conduction in molecular wires.1. A scattering formalism. *J. Chem. Phys.* 101:6849–55
100. Hamers RJ, Tromp RM, Demuth JE. 1986. Surface electronic structure of Si(111)–(7 × 7) resolved in real space. *Phys. Rev. Lett.* 56:1972–75
101. Hamers RJ. 1989. Atomic-resolution surface spectroscopy with the scanning tunneling microscope. *Ann. Rev. Phys. Chem.* 40:531–59
102. Wolkow RA. 1999. Controlled molecular adsorption on silicon: laying a foundation for molecular devices. *Ann. Rev. Phys. Chem.* 50:413–41
103. Rakshit T, Liang GC, Ghosh AW, Hersam MC, Datta S. 2005. Molecules on silicon: self-consistent first-principles theory and calibration to experiments. *Phys. Rev. B* 72:125305
104. Guisinger NP, Basu R, Baluch AS, Hersam MC. 2003. Molecular electronics on silicon: an ultrahigh vacuum scanning tunneling microscopy study. In *Molecular Electronics III*, ed. J Reimers, C Picconatto, J Ellebogen, R Shashidar, pp. 227–34. New York: N.Y. Acad. Sci.
105. Terry J, Linford MR, Wigren C, Cao RY, Pianetta P, Chidsey CED. 1999. Alkyl-terminated Si(111) surfaces: a high-resolution, core level photoelectron spectroscopy study. *J. Appl. Phys.* 85:213–21
106. Segev L, Salomon A, Natan A, Cahen D, Kronik L, et al. 2006. Electronic structure of Si(111)-bound alkyl monolayers: theory and experiment. *Phys. Rev. B* 74:165323
107. Chabal YJ. 1988. Surface infrared spectroscopy. *Surf. Sci. Rep.* 8:211–357
108. Alerhand OL, Berker AN, Joannopoulos JD, Vanderbilt D, Hamers RJ, Demuth JE. 1990. Finite temperature phase diagram of vicinal Si(100) surfaces. *Phys. Rev. Lett.* 64:2406–9
109. Nuzzo RG, Dubois LH, Allara DL. 1990. Fundamental studies of microscopic wetting on organic-surfaces. 1. Formation and structural characterization of a self-consistent series of polyfunctional organic monolayers. *J. Am. Chem. Soc.* 112:558–69
110. Hostetler MJ, Stokes JJ, Murray RW. 1996. Infrared spectroscopy of three-dimensional self-assembled monolayers: N-alkanethiolate monolayers on gold cluster compounds. *Langmuir* 12:3604–12
111. Porter MD, Bright TB, Allara DL, Chidsey CED. 1987. Spontaneously organized molecular assemblies. 4. Structural characterization of normal alkyl thiol monolayers on gold by optical ellipsometry, infrared spectroscopy, and electrochemistry. *J. Am. Chem. Soc.* 109:3559–68
112. Wang X, Colavita PE, Metz KM, Butler JE, Hamers RJ. 2007. Direct photopatterning and SEM imaging of molecular monolayers on diamond surfaces:

mechanistic insights into UV-initiated molecular grafting. *Langmuir* 23:11623–30

113. Saito N, Wu Y, Hayashi K, Sugimura H, Takai O. 2003. Principle in imaging contrast in scanning electron microscopy for binary microstructures composed of organosilane self-assembled monolayers. *J. Phys. Chem. B* 107:664–67
114. Wu YY, Hayashi K, Saito N, Sugimura H, Takai O. 2003. Imaging micropatterned organosilane self-assembled monolayers on silicon by means of scanning electron microscopy and Kelvin probe force microscopy. *Surf. Interface Anal.* 35:94–98
115. Lopez GP, Biebuyck HA, Whitesides GM. 1993. Scanning electron microscopy can form images of patterns in a self-assembled monolayer. *Langmuir* 9:1513–16
116. Wollman EW, Frisbie CD, Wrighton MS. 1993. Scanning electron-microscopy for imaging photopatterned self-assembled monolayers on gold. *Langmuir* 9:1517–20
117. Lopez GP, Biebuyck HA, Harter R, Kumar A, Whitesides GM. 1993. Fabrication and imaging of 2-dimensional patterns of proteins adsorbed on self-assembled monolayers by scanning electron microscopy. *J. Am. Chem. Soc.* 115:10774–81
118. Mack NH, Dong R, Nuzzo RG. 2006. Quantitative imaging of protein adsorption on patterned organic thin-film arrays using secondary electron emission. *J. Am. Chem. Soc.* 128:7871–81
119. Streifer JA, Colavita P, Hamers RJ. 2008. Evidence for two distinct mechanisms in photochemical grafting of molecular layers to silicon surfaces. Manuscript in preparation
120. Whelan CS, Lercel MJ, Craighead HG, Seshadri K, Allara DL. 1996. Improved electron-beam patterning of Si with self-assembled monolayers. *Appl. Phys. Lett.* 69:4245–47
121. Smith RK, Lewis PA, Weiss PS. 2004. Patterning self-assembled monolayers. *Prog. Surf. Sci.* 75:1–68
122. Kim H, Colavita PE, Metz KM, Nichols BM, Sun B, et al. 2006. Photochemical functionalization of gallium nitride thin films with molecular and biomolecular layers. *Langmuir* 22:8121–26
123. Kadyshevitch A, Naaman R. 1996. The interactions of electrons with organized organic films studied by photoelectron transmission. *Thin Solid Films* 288:139–46
124. Kadyshevitch A, Ananthavel SP, Naaman R. 1997. The role of three dimensional structure in electron transmission through thin organic layers. *J. Chem. Phys.* 107:1288–90
125. Tidswell IM, Ocko BM, Pershan PS, Wasserman SR, Whitesides GM, Axe JD. 1990. X-ray specular reflection studies of silicon coated by organic monolayers (alkylsiloxanes). *Phys. Rev. B* 41:1111–28
126. Basu R, Lin JC, Kim CY, Schmitz MJ, Yoder NL, et al. 2007. Structural characterization of 4-bromostyrene self-assembled monolayers on Si(111). *Langmuir* 23:1905–11

127. Ishizaki T, Saito N, SunHyung L, Ishida K, Takai O. 2006. Study of alkyl organic monolayers with different molecular chain lengths directly attached to silicon. *Langmuir* 22:9962–66
128. Souteyrand E, Martin JR, Martelet C. 1994. Direct detection of biomolecules by electrochemical impedance measurements. *Sens. Actuators B* 20:63–69
129. Wei F, Sun B, Guo Y, Zhao XS. 2003. Monitoring DNA hybridization on alkyl modified silicon surface through capacitance measurement. *Biosens. Bioelectron.* 18:1157–63
130. Wagner P, Nock S, Spudich JA, Volkmuth WD, Chu S, et al. 1997. Bioreactive self-assembled monolayers on hydrogen-passivated Si(111) as a new class of atomically flat substrates for biological scanning probe microscopy. *J. Struc. Biol.* 119:189–201
131. Yang WS, Hamers RJ. 2004. Fabrication and characterization of a biologically sensitive field effect transistor using a nanocrystalline diamond thin film. *Appl. Phys. Lett.* 85:3626–28
132. Yang WS, Butler JE, Russell JN, Hamers RJ. 2004. Interfacial electrical properties of DNA-modified diamond thin films: intrinsic response and hybridization-induced field effects. *Langmuir* 20:6778–87
133. Yang WS, Butler JE, Russell JN, Hamers RJ. 2007. Direct electrical detection of antigen-antibody binding on diamond and silicon substrates using electrical impedance spectroscopy. *Analyst* 132:296–306
134. Yang WS, Auciello O, Butler JE, Cai W, Carlisle JA, et al. 2002. DNA-modified nanocrystalline diamond thin-films as stable, biologically active substrates. *Nat. Mater.* 1:253–57
135. Lu MC, Knickerbocker T, Cai W, Yang WS, Hamers RJ, Smith LM. 2004. Invasive cleavage reactions on DNA-modified diamond surfaces. *Biopolymers* 73:606–13
136. Souteyrand E, Cloarec JP, Martin JR, Wilson C, Lawrence I, et al. 1997. Direct detection of the hybridization of synthetic homo-oligomer DNA sequences by field effect. *J. Phys. Chem. B* 101:2980–85
137. Cai W, Peck JR, van der Weide DW, Hamers RJ. 2004. Direct electrical detection of hybridization at DNA-modified silicon surfaces. *Biosens. Bioelectron.* 19:1013–19
138. Clare TL, Clare BH, Nichols BM, Abbott NL, Hamers RJ. 2005. Functional monolayers for improved resistance to protein adsorption: oligo(ethylene glycol)–modified silicon and diamond surfaces. *Langmuir* 21:6344–55
139. Lasseter TL, Clare BH, Abbott NL, Hamers RJ. 2004. Covalently modified silicon and diamond surfaces: resistance to nonspecific protein adsorption and optimization for biosensing. *J. Am. Chem. Soc.* 126:10220–21
140. Forbes MDE, Lewis NS. 1990. Real-time measurements of interfacial charge-transfer rates at silicon liquid junctions. *J. Am. Chem. Soc.* 112:3682–83
141. Lewis NS. 2005. Chemical control of charge transfer and recombination at semiconductor photoelectrode surfaces. *Inorg. Chem.* 44:6900–11
142. Prokopuk N, Lewis NS. 2004. Energetics and kinetics of interfacial electron-transfer processes at chemically modified InP/liquid junctions. *J. Phys. Chem. B* 108:4449–56

143. Royea WJ, Juang A, Lewis NS. 2000. Preparation of air-stable, low recombination velocity Si(111) surfaces through alkyl termination. *Appl. Phys. Lett.* 77:1988–90
144. Fajardo AM, Lewis NS. 1997. Free-energy dependence of electron-transfer rate constants at Si/liquid interfaces. *J. Phys. Chem. B* 101:11136–51
145. Fajardo AM, Lewis NS. 1996. Rate constants for charge transfer across semiconductor-liquid interfaces. *Science* 274:969–72
146. Tse KY, Nichols BM, Yang WS, Butler JE, Russell JN, Hamers RJ. 2005. Electrical properties of diamond surfaces functionalized with molecular monolayers. *J. Phys. Chem. B* 109:8523–32
147. Koiry SP, Aswal DK, Saxena V, Padma N, Chauhan AK, et al. 2007. Electrochemical grafting of octyltrichlorosilane monolayer on Si. *Appl. Phys. Lett.* 90:113118
148. Yu HZ, Morin S, Wayner DDM, Allongue P, de Villeneuve CH. 2000. Molecularly tunable "organic capacitors" at silicon/aqueous electrolyte interfaces. *J. Phys. Chem. B* 104:11157–61